RESEARCH ARTICLE

WILEY

Motor asymmetry related cerebral perfusion patterns in Parkinson's disease: An arterial spin labeling study

Song'an Shang[1] | Jingtao Wu[2] | Hongying Zhang[2] | Hongri Chen[2] |
Zhengye Cao[2] | Yu-Chen Chen[1] ® | Xindao Yin[1]

[1]Department of Radiology, Nanjing First Hospital, Nanjing Medical University, Nanjing, China

[2]Department of Radiology, Clinical Medical College, Yangzhou University, Yangzhou, China

Correspondence
Yu-Chen Chen and Xindao Yin, Department of Radiology, Nanjing First Hospital, Nanjing Medical University, No.68, Changle Road, Nanjing 210006, China.
Email: chenyuchen1989@126.com (Y.-C. C.) and y.163yy@163.com (X. Y.)

Abstract

Persisting asymmetry of motor symptoms are characteristic of Parkinson's disease (PD). We investigated the possible lateralized effects on regional cerebral blood flow (CBF), CBF-connectivity, and laterality index (LI) among PD subtypes using arterial spin labeling (ASL). Forty-four left-sided symptom dominance patients (PDL), forty-eight right-sided symptom dominance patients (PDR), and forty-five matched HCs were included. Group comparisons were performed for the regional normalized CBF, CBF-connectivity and LI of basal ganglia (BA) subregions. The PDL patients had lower CBF in right calcarine sulcus and right supramarginal gyrus compared to the PDR and the HC subjects. Regional perfusion alterations seemed more extensive in the PDL than in the PDR group. In the PDL, correlations were identified between right thalamus and motor severity, between right fusiform gyrus and global cognitive performance. None of correlations survived after multiple comparisons correction. The significantly altered CBF-connectivity among the three groups included: unilateral putamen, unilateral globus pallidus, and right thalamus. LI score in the putamen was significantly different among groups. Motor-symptom laterality in PD may exhibit asymmetric regional and interregional abnormalities of CBF properties, particularly in PDL patients. This preliminary study underlines the necessity of classifying PD subgroups based on asymmetric motor symptoms and the potential application of CBF properties underlying neuropathology in PD.

KEYWORDS
asymmetry, Parkinson's disease, perfusion imaging, regional blood flow

1 | INTRODUCTION

Parkinson's disease (PD) is a progressive neurodegenerative disorder that is characterized by movement disturbances, such as bradykinesia, resting tremor, rigidity, and postural instability (Kalia & Lang, 2015).

Unilateral onset and persisting asymmetry of these predominant motor symptoms are distinct hallmarks that differentiate PD from other types of parkinsonism and, reportedly, may be associated with contralateral dopaminergic depletion in the basal ganglia (BA) (Baumann, Held, Valko, Wienecke, & Waldvogel, 2014; Huang et al., 2017; Riederer et al., 2018). Moreover, this causative pathological change in PD could impact the cortical areas that have connections

Song'an Shang and Jingtao Wu have contributed equally to this work.

with BA. Recent studies have observed lateralization of nonmotor features dependent on motor-symptom onset in PD, exhibiting impairment of language function with right-side onset and deficits of visuospatial function with left-side onset (Lee et al., 2015; Ortelli, Ferrazzoli, Zarucchi, Maestri, & Frazzitta, 2018). Although discrepancies remain, neuroimaging studies have indicated that asymmetry in PD is in line with structural or functional changes with lateralization patterns, including gray matter volume (GMV) (Danti et al., 2015), fractional anisotropy (Knossalla et al., 2018), regional homogeneity (Huang et al., 2017), and functional activity (Wu, Hou, Hallett, Zhang, & Chan, 2015). Thus, neuroimaging studies about the alterations of BA and associated cortexes could provide new insight into the neural mechanisms underlying asymmetry in PD.

Coupled with neuronal degeneration underlying asymmetry in PD, neurovascular mechanisms, including regional metabolism or neural activity, remain undefined. PD motor- and cognitive-related patterns of abnormal metabolism have been revealed by positron emission tomography (PET) and single-photon emission computed tomography (SPECT) studies (Albrecht, Ballarini, Neumann, & Schroeter, 2019; Drzezga, 2018). Alternatively, as a safe and reproducible proxy for cerebral metabolism assessments, arterial spin labeling (ASL) is a promising MRI perfusion method that eliminates high expense, harmful radioactive materials and yields quantitative cerebral blood flow (CBF) measurements. ASL has been employed to study resting-state perfusion alterations in PD, and the results revealed that regional CBF measured by ASL was associated with disease severity and progression (Barzgari et al., 2019; Kubel, Stegmayer, Vanbellingen, Walther, & Bohlhalter, 2018; Melzer et al., 2011). Moreover, due to the essentially flat perfusion power spectrum in the resting state, ASL might be superior to blood oxygenation level-dependent functional MRI (BOLD-fMRI) in the interpretation of alterations within neural activity (Fernandez-Seara et al., 2015). Recent work has shown that the CBF-connectivity in brain regions from the same functional network may change synchronously to achieve the network's function (Havsteen, Damm Nybing, Christensen, & Christensen, 2018).

However, the alterations of regional CBF and CBF-connectivity underlying asymmetry in PD remain unclear since previous ASL-related studies scarcely took asymmetric involvement into consideration. Yamashita et al. (2017) introduced a CBF laterality index (LI) derived from ASL in BA subregions to evaluate the disease severity in PD. Nevertheless, the laterality was simply defined according to the clinical symptoms, and the formula could not afford to reflect asymmetry accurately. Therefore, the questions are raised whether lateralization in PD might influence normalized regional perfusion distribution measured by ASL, how does the CBF-connectivity observed by ASL in BA subregions alter among asymmetric patients, and whether there exists an effective CBF-related LI within BA subregions as an indicator for laterality identification. To further clarify these issues, the current study was designed to investigate aberrant CBF-associated changes in PD patients with asymmetric motor symptoms by using ASL. We hypothesized that a possible asymmetric pattern of perfusion could serve as a noninvasive in vivo biomarker related to lateralization in PD.

2 | METHODS

2.1 | Participants

From February 2019 to January 2020, 137 nondemented subjects (all right-handed Chinese individuals) were recruited through normal community health screening, newspaper advertisements, or hospital outpatient services. The idiopathic PD patients were subsequently grouped into left-sided dominance (PDL) and right-sided dominance (PDR) according to clinical laterality, including 44 (18 male and 26 female) PDL patients and 48 (22 male and 26 female) PDR patients. We enrolled 45 (22 male and 23 female) healthy controls (HCs) matched for age, gender, and years of education. This study was performed with approval from the local institutional review board of Clinical Medical College, Yangzhou University (2015KY-081), and written informed consent was obtained 24 hr prior to the examinations.

The severity and stage of PD were assessed using the Movement Disorder Society-Unified Parkinson's Disease Rating Scale III (MDS-UPDRS-III) and the H&Y scale, respectively. The levodopa equivalent daily dose (LEDD) in patients with PD was calculated as advised by Tomlinson et al. (2010). The global cognitive function of all subjects was scored using the Mini-mental State Examination (MMSE) and Montreal Cognitive Assessment (MoCA), respectively. Referring to a previous study (Prasad, Saini, Yadav, & Pal, 2018), the asymmetry index (AI) was calculated by UPDRS-III scores (items 20–26). Clinical laterality was determined by the AI and matched initial side of motor disability.

The inclusion criteria for the PD patients were as follows: (a) subjects met the United Kingdom Parkinson's Disease Society Brain Bank Clinical Diagnostic Criteria (Hughes, Daniel, Kilford, & Lees, 1992); (b) subjects were in an early clinical disease stage, H&Y stage I to II; (c) subjects confirmed side of disease onset and fulfilled at least two of the criteria of bradykinesia, rigidity, and resting tremor, or they had asymmetric resting tremor or asymmetric bradykinesia; (d) subjects had taken a stable and optimized daily dose of antiparkinsonian medications for at least 4 weeks prior to study entry. Additionally, all patients abstained from antiparkinsonian drugs for at least 12 hr prior to the clinical assessments and MRI acquisition. All subjects were required to be right-handed and have an MMSE score of ≥26.

The following exclusion criteria were used for all participants: (a) family history of PD, secondary parkinsonism, or parkinsonism syndrome; (b) any neurological disease (according to clinical assessment) such as AD, depression, dysthymic disorder, or any psychiatric disease; (c) any disease related to the nervous system, including major head injury (with loss of consciousness or other complications), cerebrovascular disorders, epilepsy, brain tumors, diabetes, alcoholism, or neurological surgery; (d) use of psychotropic agents, anticholinergic drugs or other treatments potentially interfering with cognition; (e) AI and initial side of motor disability were not matched; (f) any contraindication for MR imaging, including claustrophobia, ferromagnetic foreign bodies, and electronic implants; (g) severe vision or hearing loss; and (h) excessive head motion found in data preprocessing. The

	HC (n = 45)	PDL (n = 44)	PDR (n = 48)	F/Z value	p value
Age	58.69 ± 4.12	60.23 ± 6.49	58.83 ± 5.65	1.04	.36
Gender (M/F)	22/23	18/26	22/26	0.58	.75
Education (years)	13.80 ± 3.98	13.93 ± 3.74	13.48 ± 3.85	0.39	.83
MMSE	28.22 ± 0.92	28.61 ± 1.07	28.06 ± 1.31	4.66	.10
MoCA	27.33 ± 1.12	24.18 ± 3.64[a]	23.63 ± 3.70[a]	37.12	<.001
Course (years)	—	5.64 ± 2.98	5.31 ± 3.37	−0.74	.46
UPDRS-III	—	31.88 ± 17.68	35.64 ± 18.77	−0.89	.37
H-Y stage	—	1.63 ± 0.47	1.71 ± 0.44	−0.91	.36
LEDD (mg/day)	—	433.07 ± 42.69	420.38 ± 51.04	−1.31	.19
AI	—	−0.81 ± 0.27	0.77 ± 0.30	−8.23	<.001

Note: Data was represented as mean ± *SD*.

Abbreviations: AI, asymmetry index; F, female; HC, healthy control; H-Y, Hoehn-Yahr; LEED, levodopa equivalent daily dose; MMSE, Mini-mental State Examination; MoCA, Montreal Cognitive Assessment; M, male; PD, Parkinson disease; PDL, Parkinson with left-sided dominance; PDR, Parkinson with right-sided dominance; UPDRS, Unified Parkinson's Disease Rating Scale.

[a]Significant difference compared with HC groups (*p* < .05); *F* value for comparison among three groups (age, gender, education, MMSE, MoCA); *Z* value for comparison between PDL and PDR groups (Course, UPDRS-III, H-Y stage, LEDD, and AI).

inclusion and exclusion assessments were performed by two experienced neurologists (Yao Xu, with 31 years of experience, and Hengzhong Zhang, with 35 years of experience), who administered a structured interview to subjects and their informants. Participant demographic and clinical data are shown in Table 1.

2.2 | Data acquisition

All of the participants were scanned on a 3.0-T MRI scanner (Discovery MR750, GE Medical Systems, Milwaukee, WI) with a standard 8-channel head coil. Participants wore headphones and were instructed to lie in a supine position while keeping awake with their eyes closed and avoiding thinking of anything during the MRI scan. Participants fasted for at least 4 hr prior to the scan and withheld any medications with vasoactive properties on the day of the scan. ASL images were acquired using a background suppressed three-dimensional pseudocontinuous ASL (pCASL) sequence with the following parameters: repetition time (TR) 10.5 ms, echo time (TE) 4.9 ms, flip angle 111°, slice thickness 4 mm without gap, field of view (FOV) 240 mm × 240 mm, matrix size 128 × 128, labeling duration 1,500 ms, postlabeling delay 2025 ms, number of excitations 3, number of slices 36, 8 arms with 512 points per arm, total scan time 4 min and 44 s, units: ml/100 g/min. This sequence also included a fluid-suppressed proton density acquisition with the same image dimensions as the pCASL but without radio frequency labeling for CBF quantitation and image registration. As an anatomical reference, high-resolution T1-weighted images were acquired using a whole-brain three-dimensional brain volume imaging sequence with the following parameters: TR 12 ms, TE 5.1 ms, inversion time 450 ms, flip

angle 15°, slice thickness 1 mm, no gaps, FOV 240 mm × 240 mm, matrix size 256 × 256, voxel size 1 mm × 1 mm × 1 mm; number of slices 172, total scan time 5 min and 20 s.

2.3 | Data preprocessing and analysis

The perfusion CBF maps were calculated based on a general kinetic model for ASL using FuncTool software (version 4.6, GE Medical Systems, Milwaukee, WI) based on a general kinetic model for ASL (Ambarki et al., 2015). The ASL data were preprocessed using Statistical Parametric Mapping (SPM, version 12, https://www.fil.ion.ucl.ac.uk/spm) running in MATLAB R2016b (MathWorks Inc., Natick, MA). The detailed procedures have been described in a previous study (Okonkwo et al., 2014). Briefly, ASL images were first corrected for motion. According to the motion parameters provided by SPM, participants with translations and rotations higher than 2 mm and 2°, respectively, were removed from the analysis. Each participant's CBF image was coregistered to their structural images, and individual structural images were normalized to Montreal Neurological Institute (MNI) space; spatial transforms were concatenated to bring the CBF image to the MNI template, with resampling to a $2 \text{ mm}^3 \times 2 \text{ mm}^3 \times 2 \text{ mm}^3$ voxel size. Since normalized CBF is more sensitive for small changes in regional perfusion, the normalized CBF maps were z-scored as previously described (Melzer et al., 2011) by subtracting the global mean and dividing by the *SD*, and the z-scored CBF (z-CBF) maps were then smoothed using an 8 mm × 8 mm × 8 mm full-width at half-maximum (FWHM) Gaussian kernel. The relatively increased perfusion is interpreted as preserved perfusion relative to the global mean.

2.4 | Gray matter volume calculation

In order to correct the influence of atrophy or partial volume effects, the GMV of each voxel were taken as a covariate for statistical analysis. The GMV was calculated using SPM12. The structural MR images were segmented into white matter (WM), gray matter (GM) and cerebrospinal fluid (CSF) using the standard uniform segmentation model. After the initial affine registration of the GM concentration map to MNI space, the exponential lie algebra (DARTEL) technique was used to perform nonlinear deformation of GM concentration images and resample them to a voxel size of 1.5 mm × 1.5 mm × 1.5 mm. The GMV of each voxel was obtained by multiplying the GM concentration graph by the nonlinear determinant obtained by the spatial normalization step. Then, the GMV images were smoothed with a Gaussian kernel of 6 mm × 6 mm × 6 mm FWHM. Finally, after spatial preprocessing of the data, the normalized, modulated and smooth GMV maps were used for statistical analysis.

2.5 | CBF-connectivity analyses and LI calculation

With the assumption that PD patients with unilateral predominate motor symptoms had asymmetric perfusion impairments in BA subregions, the unilateral caudate, putamen, globus pallidus, and thalamus defined by the automated anatomical labeling (AAL) atlas (Tzourio-Mazoyer et al., 2002) were selected as seed regions of interest (ROIs). The z-CBF values for each ROI within each subject were extracted from individual z-CBF maps.

Referring to previous studies (Zhang et al., 2020; Zhu et al., 2015), for each group, ROI-based correlation analysis was used to calculate the correlation coefficient (CBF-connectivity) between each seed ROI and all other voxels of the whole brain across individuals. Gender, age, education, LEDD, and mean GMV were used as confounding covariates. Multiple comparisons were corrected using a familywise error (FWE) method ($p < .05$). The corrected CBF-connectivity maps of each group were merged into a spatial mask, where the z-CBF of each voxel was correlated with the z-CBF of the ROI in any of the three groups. To map the voxels that expressed a significantly different z-CBF correlation with each seed ROI among groups, analysis of covariance (ANCOVA) with multiple regression models was established within the spatial mask.

The LI was calculated as previously reported (Wu et al., 2015): $(L − R)/(L + R)$, in which the L and R represent the values of z-CBF in the left and right subregions, respectively. A positive LI indicates lateralization to the left side, whereas a negative LI indicates right-sided asymmetry.

2.6 | Statistical analysis

The Kolmogorov–Smirnov test was used to check the normality of clinical and demographic data distribution. One-way analysis of variance (for age) and the chi-squared (χ^2) test (for gender) were utilized to investigate the differences among groups. The continuous variables that were not normally distributed (education, disease duration, H&Y scale, MMSE score, MoCA score, UPDRS-III score, AI, LI, and LEDD) were analyzed by Kruskal–Wallis test among groups or by Mann–Whitney U test between the PDL and PDR groups. In addition, we used receiver operating characteristic (ROC) analysis to evaluate the ability of the LI to discriminate asymmetric perfusion in PD patients. Pearson correlation analysis was performed for the investigation of correlation between LI score and AI score. The above statistical analyses were performed using SPSS 19.0 software (version 19.0, SPSS Inc., Chicago, IL). A p value < .05 was considered statistically significant.

For the z-CBF and CBF-connectivity analysis, comparison of the hemispheric asymmetry among groups was performed using ANCOVA. Post hoc analysis was performed within the significant regions between groups. The above statistical analyses were performed using SPM 12 software. The nonstationary cluster-level FWE method was used to correct for ANCOVA and post hoc t test, resulting in a cluster-defining threshold of $p = .001$ and a corrected cluster significance of $p < .05$ by the FWE. The correlations between these significant regions (z-CBF value) and measurements of disease severity (UPDRS-III) and neuropsychological performance (MMSE, MoCA) in PD patients and subgroups were investigated separately using Spearman correlation analysis in SPSS 19.0 software, and $p < .05$ was defined as statistically significant. Bonferroni correction for multiple comparisons in the correlation analyses was also performed. The covariates for the above analyses included gender, age, education, LEDD, and individual mean GMV.

3 | RESULTS

3.1 | Demographic and clinical characteristics

Demographic and clinical data are summarized in Table 1. All the groups were matched for age, gender, education, and MMSE score ($p > .05$, respectively). However, the MoCA scores of the PDL and PDR groups were significantly different from those of the HC group but not different from each other ($p = .001$). The disease course and scores on the UPDRS-III, H&Y scale, and LEDD were not significantly different between the PDL and PDR groups ($p > .05$, respectively). Absolute mean values of AI that represent motor-symptom asymmetry for the PDL and PDR groups were also matched ($p > .05$).

3.2 | Group-level differences in normalized CBF

Group differences between PD patients and HC subjects are shown in Figure 1a. Relative to that of HC group, preserved perfusion was observed in the bilateral thalamus and left postcentral and precentral gyrus; decreased perfusion was found in the bilateral middle temporal gyrus (MTG), bilateral inferior temporal gyrus (ITG), bilateral middle occipital gyrus (MOG), and bilateral middle frontal gyrus (MFG).
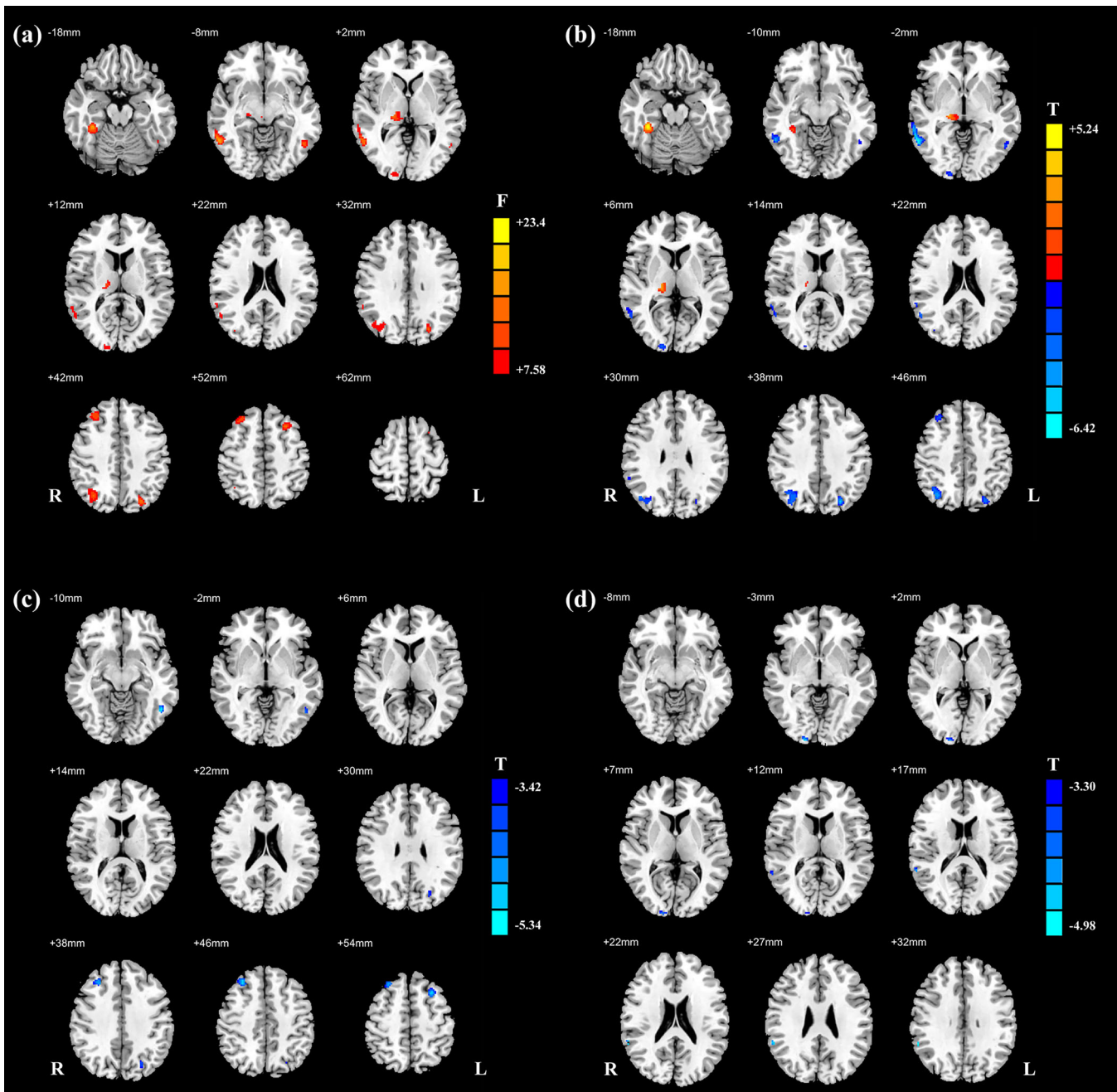
FIGURE 1 The significantly different brain regions of normalized CBF among subjects. Voxel-based analysis indicates the brain regions with significant group differences in the normalized CBF: (a) PD compared to HC; (b) PDL compared to HC; (c) PDR compared to HC; (d) PDL compared to PDR. These findings correspond to a voxel-wise height threshold of $p < .001$ (uncorrected) combined with a cluster-level extent threshold of $p < .05$ (corrected for multiple comparisons using the FWE rate). The warm color represents the significantly preserved CBF in the patients with PD. The cold color indicates that the CBF was significantly decreased in the PD patients. CBF, cerebral blood flow; HC, healthy control; PD, Parkinson disease; PDL, Parkinson with left-sided dominance; PDR, Parkinson with right-sided dominance

In the voxel-based analysis, the differences in normalized CBF among the three groups are shown in Figure 1, Tables 2 and 3. One-way ANCOVA analysis showed that significantly different regions among the HC, PDL, and PDR groups were in the right thalamus, right fusiform gyrus (FG), right calcarine sulcus, bilateral MTG, bilateral MOG, and bilateral MFG. In comparison to the HC group, PDL patients showed decreased z-CBF in the bilateral MTG, right calcarine sulcus, right supramarginal gyrus (SG), left MOG, and right MFG, while lower z-CBF in the left ITG, left MOG, and bilateral MFG was found in PDR patients. Increased z-CBF in the right fusiform gyrus and right thalamus was observed in the PDL group compared with the HC group. Furthermore, post hoc analysis also showed that PDL patients had lower z-CBF in the right calcarine sulcus and right SG compared to the PDR group.

TABLE 2 Descriptions of brain regions with significant differences by ANCOVA analysis

Brain regions (AAL)	Peak MNI coordinates (mm)			Peak F value	Cluster size (mm³)
	X	Y	Z		
Right fusiform gyrus	36	−40	−16	15.84	217
Right thalamus	18	−26	2	12.82	251
Right middle temporal gyrus	58	−56	−4	21.20	477
Right calcarine sulcus	18	−98	0	9.93	105
Right supramarginal gyrus	34	−68	44	12.61	397
Left middle occipital gyrus	−26	−76	38	15.52	176
Right middle frontal gyrus	30	32	46	12.91	236
Left inferior temporal gyrus	−50	−60	−8	12.29	133
Left middle frontal gyrus	−28	18	58	13.78	145

Note: These findings correspond to a voxel-wise height threshold of $p < .001$ (uncorrected) combined with a cluster-level extent threshold of $p < .05$ (corrected for multiple comparisons using the FWE rate). Abbreviations: ANCOVA, analysis of covariance; AAL, automated anatomical labeling; MNI, Montreal Neurological Institute.

TABLE 3 Descriptions of brain regions with significant differences by post hoc analysis

Brain regions (AAL)	Peak MNI coordinates (mm)			Peak T value	Cluster size (mm³)
	X	Y	Z		
PDL > HC					
Right fusiform gyrus	36	−38	−18	5.090	214
Right thalamus	18	−26	2	4.50	220
PDL < HC					
Right middle temporal gyrus	58	−56	−4	−5.81	473
Left middle temporal gyrus	−54	−62	−2	−3.79	60
Right calcarine sulcus	18	−98	6	−4.10	104
Right supramarginal gyrus	34	−68	44	−5.040	397
Left middle occipital gyrus	−26	−76	40	−4.99	148
Right middle frontal gyrus	32	30	46	−3.91	84
PDR < HC					
Left inferior temporal gyrus	−50	−60	−8	−5.08	98
Left middle occipital gyrus	−24	−74	34	−4.06	72
Right middle frontal gyrus	32	34	42	−4.85	197
Left middle frontal gyrus	−28	18	58	−4.86	120
PDL < PDR					
Right calcarine sulcus	20	−100	−2	−3.98	64
Right supramarginal gyrus	60	−46	22	−4.28	51

Note: These findings correspond to a voxel-wise height threshold of $p < .001$ (uncorrected) combined with a cluster-level extent threshold of $p < .05$ (corrected for multiple comparisons using the FWE rate). Abbreviations: AAL, automated anatomical labeling; CBF, cerebral blood flow; HC, healthy control; MNI, Montreal Neurological Institute; PDL, Parkinson with left-sided dominance; PDR, Parkinson with right-sided dominance.

3.3 | Correlations between z-CBF and clinical characteristics

The significant correlations (before Bonferroni correction) between the CBF changes and disease severity (UPDRS-III) or neuropsychological performance are depicted graphically in Figure 2. In the PDL group, the z-CBF values in the right thalamus were significantly positively correlated with motor severity as assessed by UPDRS-III scores ($\rho = 0.29$, $p = .027$). Additionally, we found a significantly negative correlation between the values of z-CBF in the right FG and global cognitive performance assessed by MoCA scores ($\rho = −0.37$, $p = .013$). The values of z-CBF in the other significant regions reached no significant correlations with motor severity and global cognitive performance in each PD subgroups ($\rho > 0.05$, respectively). None of correlations were
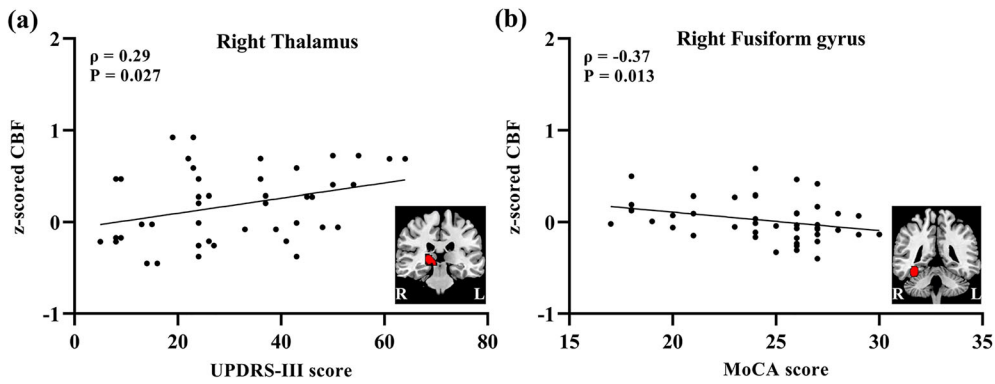
FIGURE 2 The correlations between the normalized CBF values and disease severity or neuropsychological performance. (a) Correlations between the UPDRS-III scores (*X*-axis) and the the *z*-scored CBF values of right thalamus (*Y*-axis); (b) correlations between the MoCA scores (*X*-axis) and the *z*-scored CBF values of right fusiform gyrus (*Y*-axis). CBF, cerebral blood flow; MoCA, Montreal Cognitive Assessment; UPDRS, Unified Parkinson's Disease Rating Scale
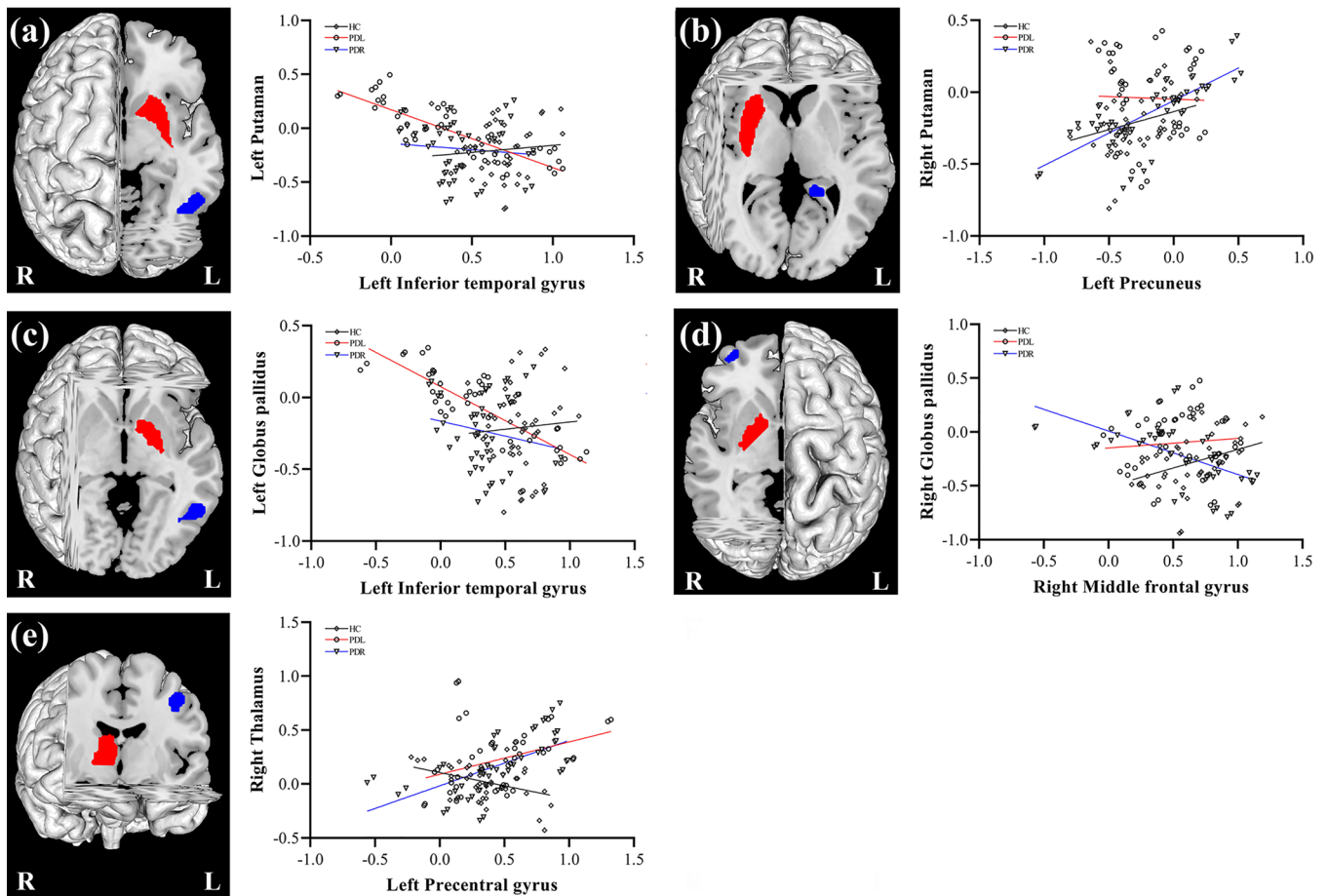

FIGURE 3 Group differences in the CBF-connectivity within BA subregions. The survived CBF-connectivity among three groups: (a) between left putamen and left inferior temporal gyrus; (b) between right putamen and left precuneus; (c) between left globus pallidus and left inferior temporal gyrus; (d) between right globus pallidus and right middle frontal gyrus; and (e) between right thalamus and right postcentral gyrus. These findings correspond to a voxel-wise height threshold of $p < .001$ (uncorrected) combined with a cluster-level extent threshold of $p < .05$ (corrected for multiple comparisons using the FWE rate). Scatter plots demonstrate the CBF-connectivity of each group (HC group-black line, PDL group-red line, PDR group-blue line). CBF, cerebral blood flow; HC, healthy control; PD, Parkinson disease; PDL, Parkinson with left-sided dominance; PDR, Parkinson with right-sided dominance

TABLE 4 Descriptions of brain regions with significant group differences in CBF-connectivity within basal ganglia subregions

Seed region	Brain regions (AAL)	Peak MNI coordinates (mm)			Peak T value	Cluster size (mm³)
		X	Y	Z		
Left putamen	*Left inferior temporal gyrus*					
	PDL < HC	−54	−56	−6	−6.032	219
	PDR < HC	−56	−58	−2	−3.77	13
	PDL < PDR	−52	−58	−10	−4.52	161
Right putamen	*Left precuneus*					
	PDR > PDL	−22	−44	0	4.53	77
	PDR > HC	−18	−44	2	5.46	86
Left Globus pallidus	*Left inferior temporal gyrus*					
	PDL < HC	−54	−56	−4	−5.58	234
	PDL < PDR	−52	−56	−10	−4.44	126
Right Globus pallidus	*Right middle frontal gyrus*					
	PDR < HC	−58	−56	−4	−3.39	3
	PDR < PDL	34	56	8	−4.30	23
Right thalamus	*Left postcentral gyrus*					
	PDR > HC	−38	−8	42	5.20	77

Note: These findings correspond to a voxel-wise height threshold of $p < .001$ (uncorrected) combined with a cluster-level extent threshold of $p < .05$ (corrected for multiple comparisons using the FWE rate).
Abbreviations: AAL, automated anatomical labeling; CBF, cerebral blood flow; HC, healthy control; MNI, Montreal Neurological Institute; PDL, Parkinson with left-sided dominance; PDR, Parkinson with right-sided dominance.

TABLE 5 Laterality index of cerebral blood flow for the basal ganglia subregions

Subregions	HC (n = 45)	PDL (n = 44)	PDR (n = 48)	F value	p value
Caudate	0.011 ± 0.099	−0.045 ± 0.18	0.052 ± 0.11	1.81	.40
Putamen	−0.028 ± 0.27	−0.20 ± 0.51[a]	0.21 ± 0.89[b,c]	8.70	.013
Globus pallidus	−0.041 ± 0.27	−0.17 ± 1.09	−0.071 ± 0.68	2.41	.30
Thalamus	−0.048 ± 1.04	−0.24 ± 0.61	−0.08 ± 0.81	4.68	.097

Note: Data was represented as mean ± SD.
Abbreviations: HC, healthy control; PDL, Parkinson with left-sided dominance; PDR, Parkinson with right-sided dominance.
[a]Significant difference between the two groups ($p < .05$).
[b]Significant difference compared with HC groups ($p < .05$).
[c]Significant difference compared with PDL groups ($p < .05$).

survived after Bonferroni correction (disease severity, $p < .0063$; neuropsychological performance, $p < .0031$). There was no significant correlation between the CBF changes and clinical characteristics was observed in PD patients ($\rho > 0.05$, respectively).

3.4 | Group differences in CBF-connectivity

Among groups, the CBF-connectivity maps with significant difference in BA subregions (bilateral putamen, bilateral globus pallidus, and right thalamus) are displayed in Figure 3 and Table 4. The surviving CBF-connectivity among the three groups after one-way ANCOVA analysis included the following: between the left putamen and left ITG, between the right putamen and left precuneus, between the left

globus pallidus and left ITG, between the right globus pallidus and right MFG, and between the right thalamus and right postcentral gyrus.

Compared with HC subjects, the PDL patients exhibited significantly decreased negative CBF-connectivity between the left putamen and left ITG, between the left globus pallidus and left ITG, and between the right globus pallidus and right MFG. The PDR patients exhibited significantly decreased negative CBF-connectivity between the left putamen and left ITG, between the right globus pallidus and right MFG, and increased positive CBF-connectivity between the right putamen and left precuneus, between the right globus pallidus and right MFG in comparison with HC subjects.

For the PDL group, significantly decreased negative CBF-connectivity between the left putamen and left ITG, between the right
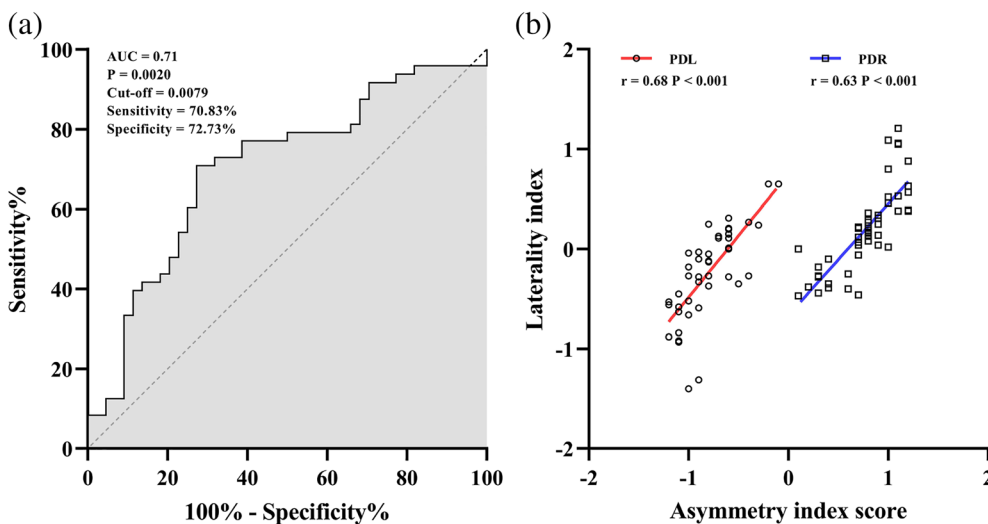
FIGURE 4 ROC curve and correlation for LI score in putamen for PDL and PDR group. (a) ROC curve of LI in putamen; (b) correlation between LI score and AI score in putamen. AI, asymmetric index; AUC, area under curve; LI, laterality index; PDL, Parkinson with left-sided dominance; PDR, Parkinson with right-sided dominance; ROC, receiver operating characteristic

putamen and left precuneus, between the left globus pallidus and left ITG, and increased negative CBF-connectivity between the right globus pallidus and right MFG were found relative to the PDR group.

3.5 | Asymmetric effect of CBF in BA subregions

The LI of CBF for the BA subregions are listed in Table 5. ROC curve of LI and correlation between LI score and AI score in putamen for PDL and PDR group are listed in Figure 4. Only the LI score in the putamen was significantly different (p = .013) among the three groups. Furthermore, the post-hoc analysis revealed that LI score was significantly different between any of the two groups (HC-PDL, p = .028; HC-PDR, p = .014; PDL-PDR, p = .010). None of the LI scores in the other subregions of the BA were significantly different among the groups (p > .05). The cross-validated area under the curve was 0.82 (95% CI 0.60–0.79, p = .0020). At a cutoff of 0.0079, for the classification between PDL and PDR group, the sensitivity and specificity were 70.83% and 72.73%, respectively. For both PD subgroups, the LI score in putamen were both positively related to that of AI score, respectively (PDL, r = .68, p < .001; PDR, r = .63, p < .001).

4 | DISCUSSION

The initial onset of motor symptoms in PD patients is primarily asymmetric and may exhibit worse side-related nonmotor symptoms during progression. In the present study, we investigated lateralized regional differences in CBF derived from ASL and obtained several central findings. (a) PDL patients experienced greater regional perfusion alterations, which were localized predominantly in the right thalamus, occipital and parietal cortex; (b) For PDL patients, dysfunction of the right thalamus in the PDL group was positively correlated with disease severity scored by UPDRS, and dysfunction of the right FG was negatively correlated with cognitive performance measured by MoCA scores; (c) There existed significant aberrant CBF-connectivity within

the unilateral putamen, unilateral globus pallidus, and right thalamus among the three groups; and (d) CBF LI in the putamen is particularly evident for assessing lateralization of PD.

4.1 | Asymmetry effects related regional perfusion changes in PD

The asymmetric symptoms of PD are frequently associated with dopaminergic depletion in contralateral BA subregions and dysfunction of connected cortical areas. Referring to the PD-related pattern (PDRP) revealed by a radiotracer study (Eidelberg, 2009), Ma et al. (2010) found an analogous PDRP of normalized CBF derived from ASL in PD patients, with preserved metabolism in the BA subregions and sensorimotor cortical regions, along with decreased metabolism in the associated cortical regions. Our results were in line with previous studies, but more specifically, we further identified preserved perfusion in the right thalamus of PDL patients in comparison to that of HC subjects, as well as a positive correlation with motor severity. The thalamus is regarded as one of the key hubs involved in striato-thalamo-cortical loops (Brooks & Piccini, 2006), and changes in regional CBF may represent excitatory or inhibitory input (Chen, Pressman, Simuni, Parrish, & Gitelman, 2015). We deduced that preserved perfusion in the right thalamus of PDL patients might be in concordance with increased inhibitory input from the subthalamic nucleus, being activated via indirect or direct pathways, as previously reported in PD (Obeso et al., 2017).

Although it is still controversial, recent studies (Barrett, Wylie, Harrison, & Wooten, 2011; Lee et al., 2015; Ortelli et al., 2018) have suggested asymmetric disruption of dopaminergic pathways to cortical areas that may progress into a lateralized cognitive pattern. A recent study (Harris, McNamara, & Durso, 2017) reported that PDL subjects may be associated with more significant cognitive decline and reduced goal-directed behavior. Our results corroborated these findings. Cognitive performance was inversely correlated with z-CBF in the right FG of PDL subjects, the regions that mainly functioned in

cognitive function, facial recognition, the visual pathway, and autonomic function. Our study indicated that altered metabolism in the right FG could be an important region involved in cognitive dysfunction in PDL patients. Rypma et al. (2015) observed that DA activity was significantly related to BOLD signals in the FG of healthy subjects by using PET and fMRI. Yao et al. (2014) reported that lower functional connectivity within the default network in PD patients was found in the right FG. Thus, an increased z-CBF in the right fusiform gyrus of PDL subjects could be interpreted as compensatory hypermetabolism in response to neurodegeneration before cognitive impairment.

The hypoperfusion of the corresponding cortex in the present study might reasonably parallel the reduction in excitatory input from the thalamus derived from dopaminergic degeneration of the nigrostriatal pathway (Dickson, 2018), coinciding with findings from previous studies (Al-Bachari et al., 2014; Barzgari et al., 2019). Since no significant differences were found between the PDL and PDR groups in attention and executive function as previously reported (Verreyt, Nys, Santens, & Vingerhoets, 2011), the distribution of hypoperfusion in MFG may be independent of asymmetric effects. Despite the prefrontal cortex, aberrant regional perfusion seemed more severe in the PDL group than in the PDR group when compared to the HC group. Previous findings (Lee et al., 2015) reported the vulnerability of right-handed PDL subjects to visuospatial and verbal dysfunctions due to possible impairments in the corresponding cortex. Compared to both the HC and PDR groups, we identified significantly decreased z-CBF in the PDL group in the right calcarine sulcus and right SG, which play crucial roles in visuospatial and language processing, respectively. However, detailed visuospatial and verbal assessments are needed in our further study to confirm this correlation.

4.2 | CBF-connectivity altered differently correlated with laterality in PD

As a physiological implication of temporally coordinated metabolism, CBF-connectivity is meaningful to evaluate functional networks within brain regions and has been applied to investigate the connectivity disorder underlying schizophrenia (Zhu et al., 2015). Here, we analyzed the altered CBF-connectivity of unilateral BA subregions involved in the pathophysiology of asymmetry in PD. We found reduced CBF-connectivity between the left ITG and the left putamen, as well as the left globus pallidus, in PD patients, which is similar to the results of other studies using BOLD (Manes et al., 2018). Interestingly, we discovered even worse connections in the PDL group when subdivisions were related to laterality. We deduced that the disruption of the lateralized CBF-connectivity pattern might be related to some distinct clinical features between PDL and PDR patients. Generally, PDR patients suffer from predominant DA depletion in the left BA subregions; thus, the increased connections for the right putamen and right thalamus in PDR patients is more likely to be suggested as compensatory for contralateral dysfunctions.

Although we found a higher connection between the right globus pallidus and right MFG in the PDL group than in the PDR group, this CBF-connectivity did not survive between PDL and HC subjects. Hence, we could still agree with the previous results (Lee et al., 2015) that there were no group differences in executive function between PD subgroups. The altered CBF connections between BA subregions and the cortex might be relatively consistent but even serious in PDL subjects with respect to PDR subjects, since no compensatory CBF-connectivity was found in our results, which needs to be verified in further studies. Unlike BOLD connectivity based on a single individual, CBF-connectivity was measured across a group of individuals, which mainly manifested the difference among groups (Zhu et al., 2015). Hence, these results reinforced the view that laterality in PD could affect CBF-connectivity; moreover, PDL subjects suffered with predominant PD pathology in the right BA regions and potentially increased metabolic stress due to right handedness in the left hemisphere (Lee et al., 2015).

4.3 | The potential of LI in the putamen for lateralization evaluation

Referring to AI, which is clinically established from UPDRS scores, several neuroimaging studies (Huang et al., 2017; Wu et al., 2015) used analogous calculations to investigate the asymmetry effects on functional impairments in the brain, but the results were unsatisfactory. As a direct reflection of regional neuronal activity, whether LI calculated from CBF could discriminate potentially among asymmetric PD patients is still rarely studied. In the current study, we found a significant LI of z-CBF in the putamen, which is classically linked to motor symptoms arising from the striato-thalamo-cortical circuit in PD. Furthermore, at a cutoff of 0.0079, this LI of z-CBF was capable of classified the lateralization of PD with optimal sensitivity and specificity. Our results provide preliminary evidence that LI of z-CBF in the putamen could serve as a perfusion biomarker for lateralization evaluation.

Several limitations in our study should be acknowledged. First, since we focused on the investigation of CBF properties between PDL and PDR groups in the early stage, we excluded PD patients without predominantly asymmetrical motor symptoms. Additionally, significant correlations did not survived after the Bonferroni correction, although our research is still meaningful to provide some enlightenment in this field. Further longitudinal studies with a larger sample size are warranted to systemically analyze aberrant perfusion in PD patients. Second, as a preliminary study, we assessed only global cognitive function. Detailed neuropsychological scales corresponding to different cognitive domains would be better for understanding the underlying mechanisms in asymmetric PD. Third, although the PD patients suspended antiparkinsonian drugs prior to the acquisition and there was no significant difference in LEDD between the subgroups of PD patients, the effect of antiparkinsonian medication still should be considered in our future investigation. Fourth, since global mean change differently between groups, intensity normalizing to all

preserved regions could be more accurate to identify the perfusion differences between groups. Finally, the CBF-connectivity is an interregional CBF correlation analysis at the group level and could not be used for additional correlation analysis with clinical measurements. This issue will be solved with the development of multidelay ASL techniques and advanced analysis.

5 | CONCLUSION

In conclusion, this preliminary study revealed that motor-symptom laterality could affect regional and interregional properties of resting-state CBF in early, nondemented PD patients. These significantly aberrant brain regions were bilateral; nevertheless, the PDL patients suffered more severe perfusion alterations within regions that were mainly involved in visuospatial dysfunctions and disease severity. The LI of the putamen could serve as an indicator for laterality classification. Our study underlines the importance of considering asymmetry in PD and highlights the potential use of CBF properties to investigate the underlying neuropathology in PD.

CONFLICT OF INTEREST
The authors report no biomedical financial interests or potential conflicts of interest.

DATA AVAILABILITY STATEMENT
The data that support the findings of this study are available on request from the corresponding author. The data are not publicly available due to privacy or ethical restrictions.

ORCID
Yu-Chen Chen https://orcid.org/0000-0002-8539-7224

REFERENCES
Al-Bachari, S., Parkes, L. M., Vidyasagar, R., Hanby, M. F., Tharaken, V., Leroi, I., & Emsley, H. C. (2014). Arterial spin labelling reveals prolonged arterial arrival time in idiopathic Parkinson's disease. *NeuroImage. Clinical*, *6*, 1–8.

Albrecht, F., Ballarini, T., Neumann, J., & Schroeter, M. L. (2019). FDG-PET hypometabolism is more sensitive than MRI atrophy in Parkinson's disease: A whole-brain multimodal imaging meta-analysis. *NeuroImage. Clinical*, *21*, 101594.

Ambarki, K., Wahlin, A., Zarrinkoob, L., Wirestam, R., Petr, J., Malm, J., & Eklund, A. (2015). Accuracy of parenchymal cerebral blood flow measurements using Pseudocontinuous arterial spin-labeling in healthy volunteers. *AJNR. American Journal of Neuroradiology*, *36*, 1816–1821.

Barrett, M. J., Wylie, S. A., Harrison, M. B., & Wooten, G. F. (2011). Handedness and motor symptom asymmetry in Parkinson's disease. *Journal of Neurology, Neurosurgery, and Psychiatry*, *82*, 1122–1124.

Barzgari, A., Sojkova, J., Maritza Dowling, N., Pozorski, V., Okonkwo, O. C., Starks, E. J., … Gallagher, C. L. (2019). Arterial spin labeling reveals relationships between resting cerebral perfusion and motor learning in Parkinson's disease. *Brain Imaging and Behavior*, *13*, 577–587.

Baumann, C. R., Held, U., Valko, P. O., Wienecke, M., & Waldvogel, D. (2014). Body side and predominant motor features at the onset of Parkinson's disease are linked to motor and nonmotor progression. *Movement Disorders: Official Journal of the Movement Disorder Society*, *29*, 207–213.

Brooks, D. J., & Piccini, P. (2006). Imaging in Parkinson's disease: The role of monoamines in behavior. *Biological Psychiatry*, *59*, 908–918.

Chen, Y., Pressman, P., Simuni, T., Parrish, T. B., & Gitelman, D. R. (2015). Effects of acute levodopa challenge on resting cerebral blood flow in Parkinson's disease patients assessed using pseudo-continuous arterial spin labeling. *PeerJ*, *3*, e1381.

Danti, S., Toschi, N., Diciotti, S., Tessa, C., Poletti, M., Del Dotto, P., & Lucetti, C. (2015). Cortical thickness in de novo patients with Parkinson disease and mild cognitive impairment with consideration of clinical phenotype and motor laterality. *European Journal of Neurology*, *22*, 1564–1572.

Dickson, D. W. (2018). Neuropathology of Parkinson disease. *Parkinsonism & Related Disorders*, *46*(Suppl 1), S30–S33.

Drzezga, A. (2018). The network degeneration hypothesis: Spread of neurodegenerative patterns along neuronal brain networks. *Journal of Nuclear Medicine: Official Publication, Society of Nuclear Medicine*, *59*, 1645–1648.

Eidelberg, D. (2009). Metabolic brain networks in neurodegenerative disorders: A functional imaging approach. *Trends in Neurosciences*, *32*, 548–557.

Fernandez-Seara, M. A., Mengual, E., Vidorreta, M., Castellanos, G., Irigoyen, J., Erro, E., & Pastor, M. A. (2015). Resting state functional connectivity of the subthalamic nucleus in Parkinson's disease assessed using arterial spin-labeled perfusion fMRI. *Human Brain Mapping*, *36*, 1937–1950.

Harris, E., McNamara, P., & Durso, R. (2017). Possible selves in patients with right- versus left-onset Parkinson's disease. *Neuropsychology, Development, and Cognition. Section B, Aging, Neuropsychology and Cognition*, *24*, 198–215.

Havsteen, I., Damm Nybing, J., Christensen, H., & Christensen, A. F. (2018). Arterial spin labeling: A technical overview. *Acta Radiologica*, *59*, 1232–1238.

Huang, P., Tan, Y. Y., Liu, D. Q., Herzallah, M. M., Lapidow, E., Wang, Y., … Chen, S. D. (2017). Motor-symptom laterality affects acquisition in Parkinson's disease: A cognitive and functional magnetic resonance imaging study. *Movement Disorders: Official Journal of the Movement Disorder Society*, *32*, 1047–1055.

Hughes, A. J., Daniel, S. E., Kilford, L., & Lees, A. J. (1992). Accuracy of clinical diagnosis of idiopathic Parkinson's disease: A clinico-pathological study of 100 cases. *Journal of Neurology, Neurosurgery, and Psychiatry*, *55*, 181–184.

Kalia, L. V., & Lang, A. E. (2015). Parkinson's disease. *Lancet*, *386*, 896–912.

Knossalla, F., Kohl, Z., Winkler, J., Schwab, S., Schenk, T., Engelhorn, T., … Golitz, P. (2018). High-resolution diffusion tensor-imaging indicates asymmetric microstructural disorganization within substantia nigra in early Parkinson's disease. *Journal of Clinical Neuroscience: Official Journal of the Neurosurgical Society of Australasia*, *50*, 199–202.

Kubel, S., Stegmayer, K., Vanbellingen, T., Walther, S., & Bohlhalter, S. (2018). Deficient supplementary motor area at rest: Neural basis of limb kinetic deficits in Parkinson's disease. *Human Brain Mapping*, *39*, 3691–3700.

Lee, E. Y., Sen, S., Eslinger, P. J., Wagner, D., Kong, L., Lewis, M. M., … Huang, X. (2015). Side of motor onset is associated with hemisphere-specific memory decline and lateralized gray matter loss in Parkinson's disease. *Parkinsonism & Related Disorders*, *21*, 465–470.

Ma, Y., Huang, C., Dyke, J. P., Pan, H., Alsop, D., Feigin, A., & Eidelberg, D. (2010). Parkinson's disease spatial covariance pattern: Noninvasive quantification with perfusion MRI. *Journal of Cerebral Blood Flow and Metabolism: Official Journal of the International Society of Cerebral Blood Flow and Metabolism*, *30*, 505–509.

Manes, J. L., Tjaden, K., Parrish, T., Simuni, T., Roberts, A., Greenlee, J. D., … Kurani, A. S. (2018). Altered resting-state functional connectivity of the putamen and internal globus pallidus is related to speech impairment in Parkinson's disease. *Brain and Behavior*, *8*, e01073.

Melzer, T. R., Watts, R., MacAskill, M. R., Pearson, J. F., Rueger, S., Pitcher, T. L., … Anderson, T. J. (2011). Arterial spin labelling reveals an abnormal cerebral perfusion pattern in Parkinson's disease. *Brain: A Journal of Neurology*, *134*, 845–855.

Obeso, J. A., Stamelou, M., Goetz, C. G., Poewe, W., Lang, A. E., Weintraub, D., … Stoessl, A. J. (2017). Past, present, and future of Parkinson's disease: A special essay on the 200th Anniversary of the Shaking Palsy. *Movement Disorders: Official Journal of the Movement Disorder Society*, *32*, 1264–1310.

Okonkwo, O. C., Xu, G., Oh, J. M., Dowling, N. M., Carlsson, C. M., Gallagher, C. L., … Johnson, S. C. (2014). Cerebral blood flow is diminished in asymptomatic middle-aged adults with maternal history of Alzheimer's disease. *Cerebral Cortex*, *24*, 978–988.

Ortelli, P., Ferrazzoli, D., Zarucchi, M., Maestri, R., & Frazzitta, G. (2018). Asymmetric dopaminergic degeneration and attentional resources in Parkinson's disease. *Frontiers in Neuroscience*, *12*, 972.

Prasad, S., Saini, J., Yadav, R., & Pal, P. K. (2018). Motor asymmetry and neuromelanin imaging: Concordance in Parkinson's disease. *Parkinsonism & Related Disorders*, *53*, 28–32.

Riederer, P., Jellinger, K. A., Kolber, P., Hipp, G., Sian-Hulsmann, J., & Kruger, R. (2018). Lateralisation in Parkinson disease. *Cell and Tissue Research*, *373*, 297–312.

Rypma, B., Fischer, H., Rieckmann, A., Hubbard, N. A., Nyberg, L., & Backman, L. (2015). Dopamine D1 binding potential predicts fusiform BOLD activity during face-recognition performance. *The Journal of Neuroscience: The Official Journal of the Society for Neuroscience*, *35*, 14702–14707.

Tomlinson, C. L., Stowe, R., Patel, S., Rick, C., Gray, R., & Clarke, C. E. (2010). Systematic review of levodopa dose equivalency reporting in Parkinson's disease. *Movement Disorders: Official Journal of the Movement Disorder Society*, *25*, 2649–2653.

Tzourio-Mazoyer, N., Landeau, B., Papathanassiou, D., Crivello, F., Etard, O., Delcroix, N., … Joliot, M. (2002). Automated anatomical labeling of activations in SPM using a macroscopic anatomical parcellation of the MNI MRI single-subject brain. *NeuroImage*, *15*, 273–289.

Verreyt, N., Nys, G. M., Santens, P., & Vingerhoets, G. (2011). Cognitive differences between patients with left-sided and right-sided Parkinson's disease. A review. *Neuropsychology Review*, *21*, 405–424.

Wu, T., Hou, Y., Hallett, M., Zhang, J., & Chan, P. (2015). Lateralization of brain activity pattern during unilateral movement in Parkinson's disease. *Human Brain Mapping*, *36*, 1878–1891.

Yamashita, K., Hiwatashi, A., Togao, O., Kikuchi, K., Yamaguchi, H., Suzuki, Y., … Honda, H. (2017). Cerebral blood flow laterality derived from arterial spin labeling as a biomarker for assessing the disease severity of parkinson's disease. *Journal of Magnetic Resonance Imaging: JMRI*, *45*, 1821–1826.

Yao, N., Shek-Kwan Chang, R., Cheung, C., Pang, S., Lau, K. K., Suckling, J., … McAlonan, G. M. (2014). The default mode network is disrupted in Parkinson's disease with visual hallucinations. *Human Brain Mapping*, *35*, 5658–5666.

Zhang, Y. N., Huang, Y. R., Liu, J. L., Zhang, F. Q., Zhang, B. Y., Wu, J. C., … Huo, J. W. (2020). Aberrant resting-state cerebral blood flow and its connectivity in primary dysmenorrhea on arterial spin labeling MRI. *Magnetic Resonance Imaging*, *73*, 84–90.

Zhu, J., Zhuo, C., Qin, W., Xu, Y., Xu, L., Liu, X., & Yu, C. (2015). Altered resting-state cerebral blood flow and its connectivity in schizophrenia. *Journal of Psychiatric Research*, *63*, 28–35.